Large scale shell model calculations for the yrast line of ^{138}Xe

IOP Conf. Series: Journal of Physics: Conf. Series **1023** (2018) 012015 doi:10.1088/1742-6596/1023/1/012015

Large scale shell model calculations for the yrast line of ^{138}Xe

S.S. Dimitrova[1], **N. Lo Iudice** [2,3]

[1]Institute of Nuclear Research and Nuclear Energy, Bulgarian Academy of Sciences, 1784 Sofia, Bulgaria
[2]Dipartimento di Fisica, Università di Napoli Federico II, Monte S. Angelo, via Cintia, I-80126 Napoli, Italy
[3]Istituto Nazionale di Fisica Nucleare, Sezione di Napoli, Monte S. Angelo, via Cintia, I-80126 Napoli, Italy

E-mail: sevdim@inrne.bas.bg

Abstract. We have adopted an importance sampling iterative matrix diagonalization algorithm to compute a large scale shell model calculation of the yrast spectrum of ^{138}Xe up to high spin thereby extending a previous calculation confined to low-lying angular momenta. An effective nucleon–nucleon interaction derived from the CD-Bonn nucleon-nucleon potential is used to compute energies, $E2$ transition probabilities, and occupation numbers. A satisfactory agreement with the experimental data is reached.

1. Introduction

The region around the doubly magic ^{132}Sn represents a precious laboratory for investigating how collectivity versus shell effects evolve as nuclei depart from shell closure and/or move away from the stability valley.

The experiments performed on several chains of nuclei including Te, Xe, Ba, and Ce isotopes [1] have been supported by theoretical investigations carried out within the quasiparticle-phonon model (QPM) (see [2] for references), large scale shell model [3, 4, 5, 6, 7], and in the nucleon pair approximation [8].

All theoretical studies were focused mainly on the quadrupole collectivity of the lowest isoscalar and mixed symmetry 2^+ states and therefore treated only low-lying levels of low spin.

We intend to explore the possibility of extending the description of the spectroscopic properties of the nuclei in this region by computing the levels of higher spins. Our attention will be concentrated first on neutron-rich even-even Xe isotopes.

These isotopes were already studied within a shell model approach endowed with an importance sampling [9] using the CD-Bonn two-body potential in a large configuration space [7]. The calculation was confined to the levels of spin up to $J^\pi = 6^+$.

Here, we adopt the same approach to generate the yrast line of ^{138}Xe up to $J^\pi = 12^+$. After a brief description of the method we analyze the results by relating them to the available experimental data.

IOP Conf. Series: Journal of Physics: Conf. Series **1023** (2018) 012015 doi:10.1088/1742-6596/1023/1/012015

2. The method

The large-scale shell model under consideration is described in [9, 10]. Here we will outline just the main steps of the algorithm.

Let us consider a symmetric matrix representing a self-adjoint operator $\hat{A}$ in an orthonormal basis $\{\mid 1\rangle, \mid 2\rangle, \ldots, \mid N\rangle\}$. In order to determine the lowest m eigenvectors of the matrix we have to follow an initialization loop and a subsequent set of refinement loops.

*Step 1.*The initialization begins by diagonalizing the matrix (a_{ij}) (i,j $= 1,$n), where n fulfills the relation $(m < n \ll N)$. We choose the lowest m eigenvalues λ_i and eigenvectors $\mid \phi_i\rangle$, and constructing the new matrix of dimensions $(m + n')$

$$\alpha = \begin{pmatrix} \lambda & b_j \\ b_j & a' \end{pmatrix} \quad , \tag{1}$$

where $\{\lambda\}$ is a diagonal block composed of the eigenvalues $(\lambda_i^n, i = 1, m)$, a' is the new submatrix $a'_{jj'} = \langle j \mid \hat{A} \mid j'\rangle$ with $(j, j' = n + 1, n')$, and $\{b_j\}$ is an off-diagonal block connecting λ to a and is composed of the elements $b_{ij} = \langle\, \phi_i^n \mid \hat{A} \mid j \,\rangle$ where $(i = 1, m;\ j = n + 1, n')$.

We add the lowest m eigenvalues $\lambda_i^{n'}$ together with the corresponding eigenvectors $\mid \phi_i^{n'}\rangle$ to a new subset of orthonormal states $\mid j\rangle$ to build a new matrix and proceed as we did for α. This initialization loop ends when the whole configuration space is exhausted. As a result, a zero order approximation to the lowest eigenvalues and eigenvectors is obtained

$$E_i^{(0)} \equiv \lambda_i^N, \quad \mid \psi_i^{(0)}\rangle \equiv \mid \phi_i^N\rangle = \sum_{j=1}^{N} c_j^{(N)} \mid j\rangle \quad , \quad \{i = 1, m\}. \tag{2}$$

Step 2. The solutions of the eigenvalue Eqs. (2) are used as an entry to the first refinement loop, which goes through the same steps as described above with one difference. One should just solve an eigenvalue problem of general form since the vectors $\mid \phi\rangle$ and $\mid j\rangle$ are no longer orthogonal. It has been shown in [9] that the eigenvalues $E^{(n)}$ and eigenvectors $\mid \psi^{(n)}\rangle$ obtained after the n-th loop converge to the solution of the exact diagonalization of $\langle \hat{A}\rangle$.

Step 3. The implementation of the method requires an adequate sampling criterion for reducing the size of the configuration space. Bearing in mind that the algorithm provides accurate solutions already after the initialization loop, one can sample the configuration space as follows:

- Diagonalize the submatrix $\{a_{ij}\}\,(i, j = 1, m)$ and obtain its eigenvalues λ_i;
- For $j = m + 1, \ldots, N$, diagonalize the $m + 1$-dimensional matrix

$$\alpha = \begin{pmatrix} \Lambda_m & \vec{b}_j \\ \vec{b}_j^T & a_{jj} \end{pmatrix}, \tag{3}$$

  where $\vec{b}_j = \{b_{1j}, b_{2j}, \cdot, b_{mj}\}$.

- Accept the new state only if

$$\sum_{i=1,m} \mid \lambda'_i - \lambda_i \mid > \epsilon \quad , \tag{4}$$

  otherwise ignore the state and continue the sampling process with a new vector j. In the relation above ϵ is a small parameter which allows to control the accuracy of the truncation. In the actual calculations we use an upgraded important sampling procedure [11, 12].

The main advantage of the method is that the two key elements – the diagonalization procedure and the importance sampling– are closely related. The algorithm provides robust and always ghost–free solutions and the accuracy of the truncation procedure is fully under control.

3. Calculations

We will describe ^{138}Xe as ^{132}Sn core plus four valence protons in the $(1g_{7/2},d_{5/2},2d_{3/2},1h_{11/2},3s_{1/2})$ model space and two valence neutrons occupying the $(2f_{7/2},3p_{3/2},1h_{9/2},3p_{1/2},2f_{5/2},1i_{13/2})$ levels. The effective two–body potential is a renormalized G matrix [13] derived from the CD–Bonn potential [14]. The single-particle energies are the same as in [7]. They are listed in Table 1.

Table 1. Single particle energies in MeV.

Protons		Neutrons	
$1g_{7/2}$	0.00	$2f_{7/2}$	0.00
$2d_{5/2}$	0.96	$3p_{3/2}$	0.85
$2d_{3/2}$	2.71	$1h_{9/2}$	1.56
$1h_{11/2}$	2.80	$3p_{1/2}$	1.66
$3s_{1/2}$	3.50	$2f_{5/2}$	2.00
		$1i_{13/2}$	2.11

In the previous calculation [7] scaling factors for the pairing-like components of the two–body potential were adopted. For the optimal reproduction of the experimental values of the excitation levels up to $J^\pi = 12^+$ for ^{138}Xe [15] we need to scale just the proton–proton $J^\pi = 0^+$ components by the factor 0.85.

We perform the shell model calculations in the m–scheme. It is useful to replace the standard two–body Hamiltonian by the modified one

$$H = H + \alpha[\hat{\mathbf{J}}^2 - J(J+1)] \quad , \tag{5}$$

where α is a positive constant. Due to the additional term, the states with total spin different from J are pushed up in energy for a sufficiently large α. Thus, the diagonalization yields only the low-lying states of a given spin J.

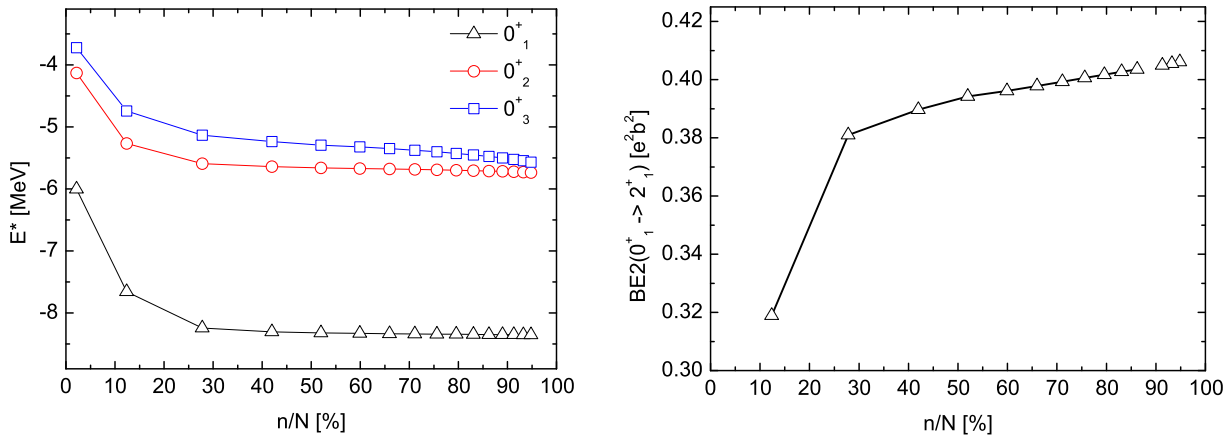

Figure 1. Convergence of the energy of the lowest 0^+ states in MeV and the BE2$(0_1^+ \rightarrow 2_1^+)[e^2fm^4]$ value in ^{138}Xe.

Although the shell model problem for ^{138}Xe does not need a severe truncation of the configuration space for any J value, the importance sampling procedure described in Sect. (2)

will be absolutely necessary for the heavier xenon isotopes. Thus we will use the importance sampling to restrict the size of the Hamiltonian and to study the convergence of the method.

First we determine a series of small positive values $\{\epsilon_1 > \epsilon_2 > ... > \epsilon_m\}$ and used them as a sampling criterion in Eq. (4). To each value of ϵ corresponds an unique number of configuration states which determine the Hamiltonian matrix to be diagonalize.

In Fig.1 we present the behavior of the energies of the lowest $J^\pi = 0^+$ states (left panel) and the value of the B($E2; 0_1^+ \rightarrow 2_1^+$) (right panel) as functions of the size of the Hamiltonian matrix. It is worthwhile to mention that, during the sampling procedure, all possible configurations are explored. The eigenvalues of the lowest $J^\pi = 0^+$ states and the B(E2) value have a steep exponential trend and, then, tend to their asymptotic values. The energies, however, converge to the exact eigenvalues with just a small fraction of basis states. The convergence of the $E2$ transition rate is considerably slower. The reason for this is that the sampling is based mostly on the energies.

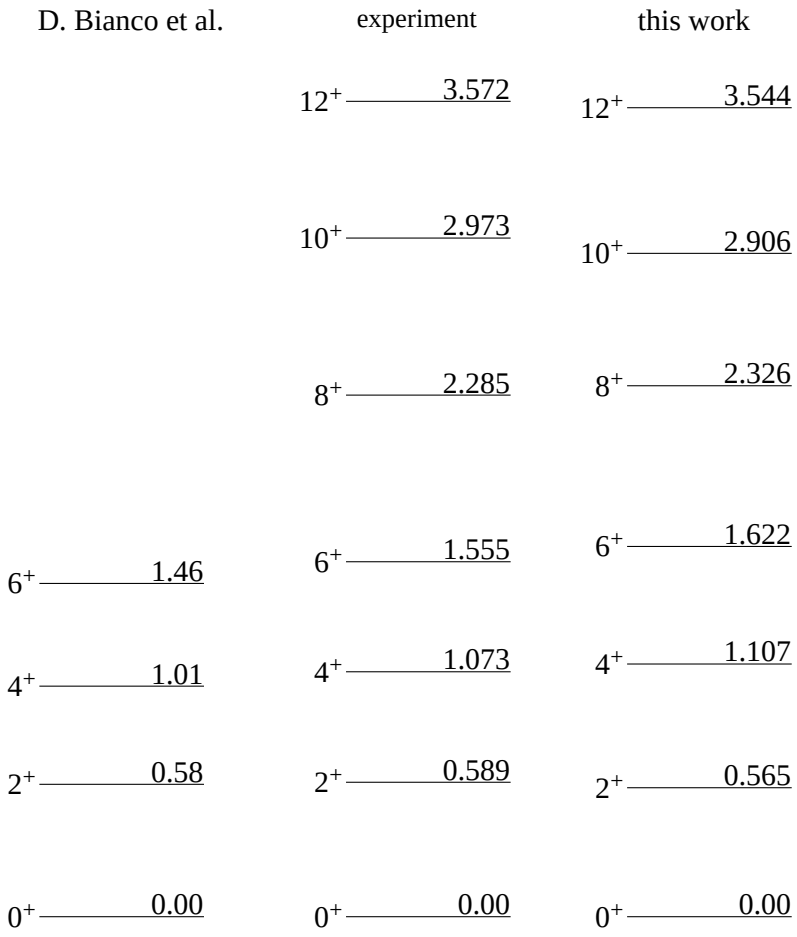

Figure 2. Low energy spectrum of ^{138}Xe in MeV, compared with the experimental data [15] and the previous calculation [7].

4. Results

The energy spectrum of ^{138}Xe is presented in Fig.2. A very good agreement with the experimental data [15] is achieved for the low lying excited states as well as for levels up to

$J^\pi = 12^+$.

Table 2 shows that the calculation reproduces also the experimental $E2$ transition rate [16] improving slightly the previous result [7]. In both cases the adopted effective charges were $e_\pi = 1.6e$ and $e_\nu = 0.7e$.

Table 2. Experimental and theoretical BE2($0_1^+ \rightarrow 2_1^+$)$[e^2b^2]$.

Exp [16]	Bianco [7]	this work
0.40 (10)	0.379	0.406

A further insight into the shell structure of the nucleus is provided by the proton and neutron occupation numbers listed in Table 3. One should notice that our values deviate significantly from the independent particle model rule ($2(j+1)$ for the hole and 0 for the particle states).

There is a large depletion of the proton Fermi sea starting from 0.52 for the 0^+ ground state and decreasing to 0.45 for the first 12^+ state. This means that the excited states are highly correlated. For neutrons, the depletion is considerably smaller. There is also no dependence on the spin of the excited states as for protons.

5. Conclusions

The calculation has shown that the importance sampling algorithm can be extended successfully to high spin states at least in ^{138}Xe. It is, in fact, able to reproduce the yrast line up to $J^\pi = 12^+$ as well as the available experimental $E2$ transition rate The present work is the first step of a project intended to cover low and high spin spectra of the nuclei in the region around ^{132}Sn.

Table 3. Occupation numbers of the single particle levels for ^{138}Xe.

	0_1^+	2_1^+	4_1^+	6_1^+	8_1^+	10_1^+	12_1^+
protons							
$1g_{7/2}$	1.929	1.928	1.960	1.978	1.984	2.077	2.195
$2d_{5/2}$	1.429	1.426	1.431	1.463	1.515	1.464	1.390
$2d_{3/2}$	0.323	0.336	0.331	0.304	0.283	0.278	0.248
$1h_{11/2}$	0.177	0.144	0.118	0.107	0.052	0.032	0.036
$3s_{1/2}$	0.140	0.165	0.159	0.147	0.164	0.148	0.130
depletion	0.52	0.52	0.51	0.50	0.50	0.48	0.45
neutrons							
$2f_{7/2}$	1.241	1.101	1.140	1.232	1.088	1.124	1.165
$3p_{3/2}$	0.342	0.492	0.418	0.316	0.400	0.351	0.223
$1h_{9/2}$	0.096	0.075	0.077	0.094	0.146	0.128	0.213
$3p_{1/2}$	0.098	0.126	0.149	0.096	0.124	0.136	0.067
$2f_{5/2}$	0.176	0.181	0.198	0.243	0.225	0.247	0.322
$1i_{13/2}$	0.046	0.024	0.016	0.016	0.016	0.014	0.009
depletion	0.38	0.45	0.43	0.38	0.46	0.44	0.42

Acknowledgments
This work is partly supported by the DFNI-T02/19 grant of the Bulgarian Science Fond. This financial support is gratefully acknowledged.

References

[1] C. Bauer *et al.* Phys. Rev. C **88**, 021302(R) (2013) and references therein.
[2] N. Lo Iudice, V. Y. Ponomarev, C. Stoyanov, A. V. Sushkov, and V. V. Voronov, J. Phys. G: Nucl. Part. Phys. **39**, 043101 (2012).
[3] N. Shimizu, T. Otsuka, T. Mizusaki, and M. Honma, J. Phys. Conf. Ser. **49**, 178 (2006).
[4] K. Sieja, G. Martnez-Pinedo, L. Coquard, and N. Pietralla Phys. Rev. C **80**, 054311 (2009).
[5] D. Bianco, F.Andreozzi,N. Lo Iudice, A. Porrino, and F.Knapp, Phys. Rev. C **85**, 034332 (2012).
[6] D. Bianco,N. Lo Iudice, F. Andreozzi,A. Porrino, and F.Knapp, Phys. Rev. C **86**, 044325 (2012).
[7] D. Bianco,N. Lo Iudice, F. Andreozzi,A. Porrino, and F.Knapp, Phys. Rev. C **88**, 024303 (2013).
[8] L. Y. Jia, H. Zhang, and Y. M. Zhao, Phys. Rev. C **75**, 034307 (2007).
[9] F. Andreozzi, A. Porrino and N. Lo Iudice, J. Phys. A **35**, L61 (2002).
[10] F. Andreozzi, N. Lo Iudice and A. Porrino, J. Phys. G **29**, 2319 (2003).
[11] D. Bianco, F. Andreozzi, N. Lo Iudice, A. Porrino and F. Knapp, J. Phys. G: Nucl. Part. Phys. **38**, 025103 (2011).
[12] D. Bianco, F. Andreozzi, N. Lo Iudice, A. Porrino and S. Dimitrova, J. Phys.: Conference Series **205**, 12002 (2010);
[13] M. Hjorth-Jensen, T. T. Kuo, and E. Osnes, Phys. Rep. 261, 125 (1995).
[14] R. Machleidt, Phys. Rev. C **63**, 024001 (2001).
[15] Jun Chen, Nucl. Data Sheets **146**, 1 (2017)
[16] Th. Kröll et al., Eur. Phys. J. Special Topics **150**, 127 (2007).